Logic Networks Based on Immunorecognition Processes

Guinevere Strack,[†] Soujanya Chinnapareddy,[†] Dmytro Volkov,[‡] Jan Halámek,[†] Marcos Pita,[†] Igor Sokolov,*[,‡,§] and Evgeny Katz*[,†,§]

Department of Chemistry and Biomolecular Science, Department of Physics, and Nanoengineering and Biotechnology Laboratories Center (NABLAB), Clarkson University, Potsdam, New York 13699

Received: June 15, 2009

The biochemical system logically processing biochemical signals using immune-specific and biocatalytic reactions was designed, and the generated output signals were analyzed by AFM and optical means. Different patterns of immune signals resulted in the formation of various interfacial structures followed by biocatalytic reactions activated by the next set of biochemical inputs. The developed approach to multisignal biosensing allows qualitative evaluation of the biochemical information in terms of **YES−NO**, providing the base for novel molecular-level logic analysis of complex patterns of biochemical signals. Application of AFM to read out the structures generated on the interface could potentially lead to substantial miniaturization of the immune logic systems.

Introduction

Biomolecular computing,[1] being a subarea of unconventional chemical computing,[2] is aiming at the chemical information processing using biochemical means instead of electronics. Biomolecular components of the information processing systems can include proteins/enzymes,[3] DNA,[4] RNA,[5] and whole biological cells.[6] Two different branches of the biocomputing systems are developing in different directions. One is aiming at competing with traditional electronic computation using advantages of parallel computing performed by numerous biomolecules (usually represented by DNA computing).[4] This is expected to solve complex combinatorial problems faster and more effectively than conventional computers.[7] Another direction is not aiming at any complex computation but rather creating a "smart" information processing interface between biological and electronic systems, operating as a logic information preprocessing unit. Biocomputing logic gates and their networks were functionally integrated with conducting electrodes,[8] Si-based chips,[9] and even complex bioelectronic devices (e.g., biofuel cells)[10] to process multiple biochemical signals and to logically control the states of the electronic systems. Alternatively, biomolecular computing units can interface biological systems and signal-responsive materials functioning as "smart" chemical actuators.[11] Systems of even moderate complexity could effectively process several biochemical signals according to the built-in "program". This research direction was pioneered recently and based on the application of enzyme-catalyzed reactions.[12] Various logic gates (**AND**, **OR**, **XOR**, **NOR**, **INHIB**, etc.) were developed based on solely enzymatic systems. Experimental and theoretical work has demonstrated the possibility to scale up their complexity, reaching enzyme logic networks composed of several concatenated logic gates operating in a concerted way and processing multiple biochemical signals.[13,14] The biochemical networks could demonstrate robust error-free operation upon appropriate optimization of their components and interconnections.[14] However, the limit of the biocomputing network complexity is set by the cross-reactivity of the enzyme-catalyzed reactions. Only enzymes belonging to different biocatalytic classes (oxidases, dehydrogenases, peroxidises, hydrolases, etc.) could operate in a single "soup" without significant cross-reactivity. If chemical reasons require the use of cross-reacting enzymes in the system, they must be compartmentalized using patterning on surfaces or microfluidic devices. Application of more selective biomolecular interactions would be an advantage to make biocomputing systems more specific to various input signals and less cross-reactive in the chemical signal processing. The present paper represents the first attempt to develop logic gates and their networks based on immune recognition processes, assuming their high selectivity and specificity, which would allow further increase of the complexity of the biocomputing information processing.

It should be noted that there is a major difference of the developed approach from what has already been called "immunologic" in relation to the analysis of data obtained in immune-responsive sensors (for example, ELISA readers).[15] Each sensitive element of an immunosensor is responsible for the detection of a single antibody or antigen. The information collected from multiple sensitive elements of the immune sensors is processed by means of special algorithms implemented in regular digital computers. Here we propose to join multiple sensitive elements into one single element, which will be responsive to multiple inputs either antibodies or antigens and even other enzyme-sensitive "inputs". The information coming from multiple signals is processed through a built-in logic directly on the molecular level. This logic can be implemented via reading optical outputs[12−14] (UV-VIS absorbance spectra or fluorescent signal) or force signatures[16] (by means of atomic force microscopy, AFM).[17] Both approaches are demonstrated in the present work. It is worth mentioning that there is an intriguing feature of using the AFM method of detection. Using AFM, we demonstrated that in our method the affinity of the antibodies can reliably be detected on the area as small as $\sim 3\ \mu m^2$. This can lead to substantial miniaturization of the immune logic systems. The developed immune logic can

* To whom correspondence should be addressed. Fax: 1-315-268-6610. Tel.: 1-315-268-2375. E-mail: isokolov@clarkson.edu (I.S.); Tel.: 1-315-268-442. E-mail: ekatz@clarkson.edu (E.K.).
† Department of Chemistry and Biomolecular Science.
‡ Department of Physics.
§ Nanoengineering and Biotechnology Laboratories Center.

10.1021/jp905620c CCC: $40.75
Published on Web 08/11/2009

further be complemented by the enzymatic logic[12−14] mentioned above. An example involving glucose oxidase is demonstrated here.

Experimental Section

Chemicals and Reagents. Glucose oxidase (GOx) from *Aspergillus niger* type X-S (E.C. 1.1.3.4), β-D-(+)-glucose (99.5% GC), antinitrotyrosine IgG from rabbit (anti-NT), 2,4-dinitrophenyl modified human serum albumin (DNP−HSA; ∼35 DNP species per protein), bovine serum albumin (BSA), 3,3′,5,5′-tetramethylbenzidine (TMB), 3-nitro-L-tyrosine ethyl ester hydrochloride, *N*-(3-dimethylaminopropyl)-*N*′-ethylcarbodiimide hydrochloride (EDC), and (4-(2-hydroxyethyl)-1-piperazineethanesulfonic acid (HEPES) were purchased from Sigma−Aldrich. Antidinitrophenyl IgG polyclonal (anti-DNP) from goat was purchased from Oxford Biomedical. Mouse origin IgG against goat immunoglobulin and IgG specific against rabbit IgG, both labeled with HRP (antigoat-IgG-HRP and antirabbit-IgG-HRP, respectively), were purchased from Jackson Immuno. All commercial chemicals were used as supplied without further purification. The nitrotyrosine−BSA conjugate (NT−BSA; ∼60 NT species per protein) was prepared via standard carbodiimide coupling (see Supporting Information for details). Ultrapure water (18.2 MΩ·cm) from a NANOpure Diamond (Barnstead) source was used in all of the experiments.

Preparation of the Logic Gate's "Machinery" and Definition of the Input Signals. The 96 well polystyrene ELISA microtiter plates (VWR) served as the immuno-based logic system, with each well functioning as a digital processing reservoir. The antigen conjugate mixtures (DNP−HSA and NT−BSA), in the protein ratio of 1:1 (10 $\mu g \cdot mL^{-1}$ each conjugate), were prepared in 0.05 M carbonate buffer, pH 9.6, deposited on the ELISA plate (100 μL per well) and incubated overnight at 4 ± 2 °C to adsorb on the surface of the well. The excess antigen was removed by washing each well four times with 300 μL of phosphate-buffered saline (PBS) with Tween-20 (PBST) (137 mM NaCl, 2.7 mM KCl, 10 mM Na_2HPO_4, and 1.76 mM KH_2PO_4, pH = 7.4 with 0.05% (v/v) Tween-20). The blocking step (to prevent nonspecific adsorption of antibodies) was accomplished via the addition of 300 μL of blocking solution (10 $mg \cdot mL^{-1}$ BSA dissolved in PBS) to each antigen-coated well. The excess BSA was removed after 1 h of incubation at 25 ± 2 °C by washing each well four times with PBST, yielding the antigen-functionalized surface. The primary antibodies, anti-DNP and anti-NT, were applied as input signals (**A** and **B** signals, respectively) to the antigen-functionalized surface. The absence of the antibodies was considered as the logic input **0**, while their optimized concentrations of 2 $\mu g \cdot mL^{-1}$ for anti-DNP and 0.1 $\mu g \cdot mL^{-1}$ for anti-NT were defined as logic input **1**. For further protection against the nonspecific binding of the antibodies to the well surface, 1 $mg \cdot mL^{-1}$ BSA in PBST was added to the antibody solutions. The input signals (antibody solutions, 100 μL) were applied in all four combinations to separate wells **0**,**0**; **0**,**1**; **1**,**0**; and **1**,**1** (where the first notation corresponds to signal **A** and the second to signal **B**) and reacted with the modified surface for 1 h at 25 ± 2 °C. Afterward, the surfaces of the wells were washed again with the PBST solution. After reacting the antigen-functionalized wells with the antibody signals, the surface was treated with a mixture of secondary antibodies, antigoat-IgG-HRP and antirabbit-IgG-HRP (0.05 $\mu g \cdot mL^{-1}$ each antibody), with 1 $mg \cdot mL^{-1}$ BSA in PBST buffer (100 μL) for 1 h at 25 ± 2 °C. After the incubation, the plate was washed four times with the PBST solution to remove the excess secondary antibodies. The generated surface was used to analyze optical output signals in the presence of GOx, 3.6 units·mL^{-1}, and TMB, 41.6 μM, in 50 mM citrate buffer, 300 μL, pH 5.0, (being parts of the logic system "machinery"), while glucose and O_2 were applied as additional input signals (**C** and **D** signals, respectively). The absence of glucose and O_2 was considered as the input signal **0**, while 1 mM glucose and O_2 in equilibrium with air were defined as the input signal **1**. For the experiments done in the absence of oxygen (signal **D** is **0**), the reaction solution contained also Na_2SO_3, 100 mM, as an oxygen-depleting agent. Absorbance of the biocatalytically oxidized TMB was measured at $\lambda = 655$ nm after reacting for 20 min using a BIO RAD Model 680 ELISA microplate reader.

Atomic Force Microscopy. A Nanoscope IIIa MultiMode (Digital Instruments/Veeco, Inc., Santa Barbara, CA) atomic force microscope (AFM) was used in the present study. A standard cantilever holder for operation in liquids was employed. To collect sufficient statistics, the force−volume mode of operation was utilized, providing information about both the surface topography and the force curves simultaneously. The force curves were collected over at least five areas of 1 μm^2 each. The AFM probe moved up and down during the force collection with a frequency of 2 Hz. The AFM software used was version 5.12, release 4. A JV scanner was used. The samples for analysis were prepared on the cut 6 mm bottoms of a functionalized polystyrene microtiter plate. The plate bottoms were cleaned via ultrasonication in ultrapure water for 15 min. The water was replaced, and the sonication was repeated two more times. The modification procedure of the plate bottoms was congruous with the previously described steps. All force measurements were performed in PBS.

Results and Discussion

The biomolecular logic system based on immune-selective recognition of input signals was designed similarly to a standard "sandwich"-type immunosensor on a commercial ELISA plate, using a mixed thin film of two different antigens, as shown in Scheme 1. Two antigens, 2,4-dinitrophenyl (DNP) and 3-nitro-L-tyrosine (NT) bound to the carrier proteins HSA and BSA, respectively, were physically adsorbed on polystyrene wells of an ELISA plate. The surface functionalized with the mixed film of antigens, DNP−HSA and NT−BSA, was reacted with the first set of the biomolecular input combinations. The corresponding primary antibodies, anti-DNP and anti-NT, were applied as the input signals. Their absence was considered as the logic **0** input signal, while their optimized concentrations, 2 and 0.1 $\mu g \cdot mL^{-1}$ for anti-DNP and anti-NT, respectively, were defined as the **1** logic inputs. The biomolecular input signals were applied in four different combinations, **0**,**0**; **0**,**1**; **1**,**0**; and **1**,**1**, where the first digit corresponds to the anti-DNP input (signal **A**) and the second digit means the anti-NT input (signal **B**). After this step, four different surface structures were generated corresponding to the absence of both antibodies, the presence of one of them (anti-DNP or anti-NT), or the presence of both of them. All possible configurations originating from this step were further reacted in a similar way with a mixture of secondary antibodies labeled with a biocatalytic tag (antigoat-IgG-HRP, 0.05 $\mu g \cdot mL^{-1}$, and antirabbit-IgG-HRP, 0.05 $\mu g \cdot mL^{-1}$) specific to the primary antibodies on the surface.

To demonstrate the reading of the above signals, we used either force or optical measurements. The former were done by means of AFM. Apart from the straightforward detection of the physical presence of the attached molecules, the AFM allowed us to test the surface homogeneity of the assembled molecular

SCHEME 1: Assembling and Operation of the Immune Enzyme Logic System Activated by Four Input Signals

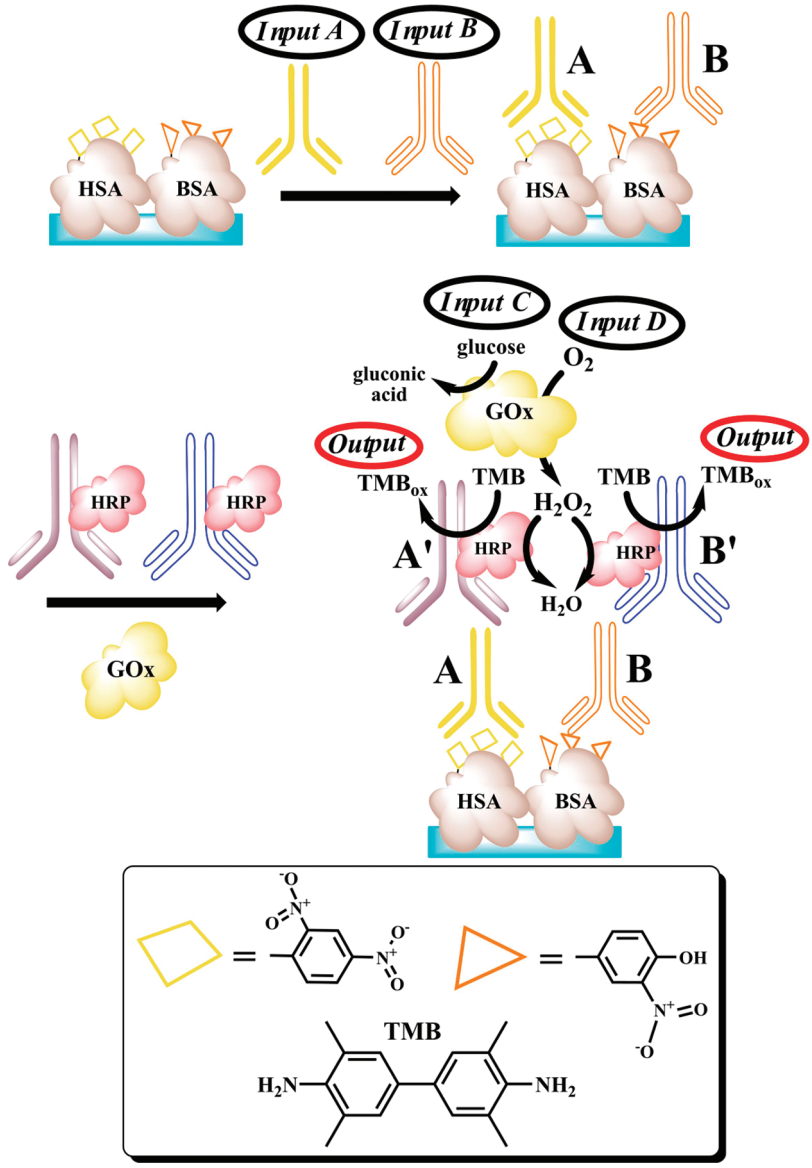

structure. This is important because we are dealing with an intrinsically heterogeneous system of different molecules, including two different antigens assembled on a surface. Moreover, the assembly of molecule layers is heterogeneous in nature. Defects and domains are intrinsic to this process. Here, we used AFM to test each step of the molecular "machinery" assembling described above, over five randomly chosen areas of 1 μm^2 each. The molecular response was analyzed with 256 points equally distant within each 1 μm^2 area. The results of these measurements are shown in Figure 1.

There are four cases analyzed with the AFM generated upon application of **0**,**0**; **0**,**1**; **1**,**0**; and **1**,**1** input signal combinations. In principle, the force dependences could be analyzed in terms of the grafting density and the length of the attached molecules.[16,17] However, this is beyond the scope of the present work and will be published elsewhere. To identify the presence of the molecular layers, we can quantitatively define it as an AFM tip−surface distance when the molecular layer produces the "resistance" force of, say, 0.5 nN. It should be noted that this threshold number is taken to be almost arbitrary. However, it approximately corresponds to the thickness of a brush layer if we use the brush model.[16] Secondly, this definition is sufficient to unambiguously detect the presence of antibodies with the AFM. Figure 2 shows the averages and standard distributions of the thickness of the molecular layers averaged over three areas for each of the four cases shown in Figure 1. One can conclude that these thicknesses are statistically significantly different (at $p > 0.08$ level, ANOVA test). Because the signal corresponding to the presence of antibodies shown in Figure 2 is the average over three areas of 1 μm^2 each, one can conclude that the signal can be detected from an area as small as 3 μm^2.

Analyzing the output signals presented in Figure 2, one can see that for the cases of the **0**,**1** and **1**,**0** input combinations, the output signals follow the response pattern expected for the **OR** logic gate activated by the immune signals **A** and **B**. In the case of **1**,**1**, the response can obviously be defined as **YES** as well. In principle, one could define this signal as a separate result/output. However, this would imply a much richer logic than binary. This is beyond the scope of the present approach. It is worth noting that the output signal in the case of **1**,**1** inputs is not a trivial doubling of the number of antibodies. As was described above, the total density of antigens stays the same for all four cases. As such, the nature of a quite high output signal for the **1**,**1** input combination is not entirely clear.

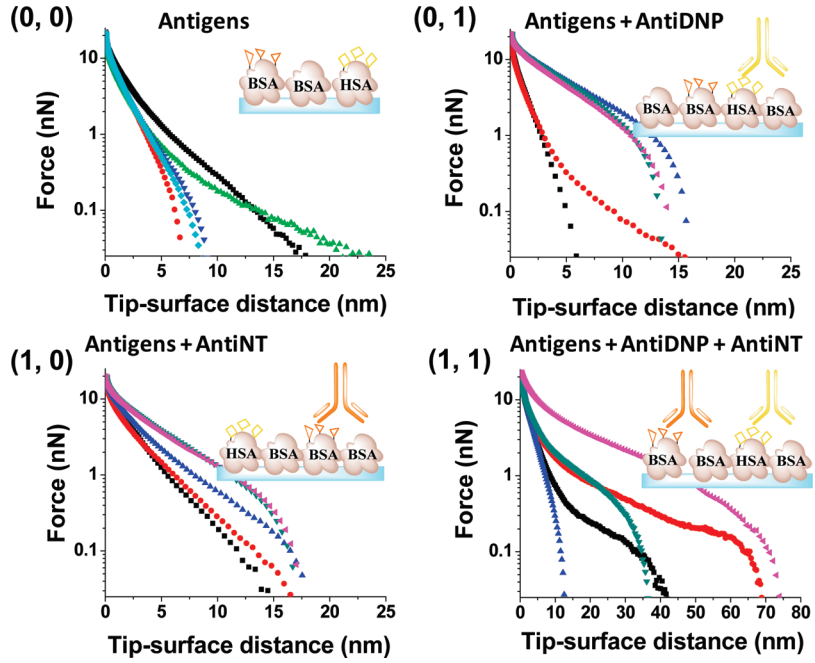

Figure 1. Force dependences measured over the surfaces of different molecular assembles. Each force curve is an average of approximately 200 force curves measured over an area of 1 μm^2. Force dependences are shown for five different areas for each case.

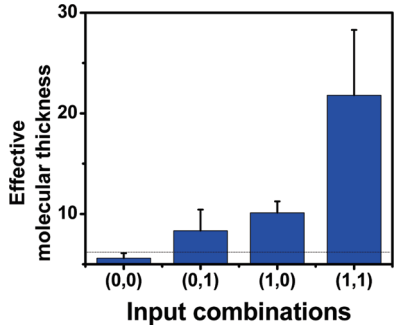

Figure 2. The average molecular thickness calculated for different input combinations. The average was done over five areas, 1 μm^2 each. The dash line shows the threshold separating the digital **0** and **1** output signals produced by the system.

Below, we demonstrate the use of optical methods. It was interesting to make a further step and implement enzymatic logic in addition to the demonstrated immune-based logic. Then, GOx, 3.6 mg·mL^{-1}, and TMB, 41.6 μM, were added to the solutions in all wells, being parts of the logic network "machinery". At this point, the biomolecular logic system was ready to accept the next set of biochemical input signals, glucose (input **C**) and O_2 (input **D**). The absence of them was considered as the logic value **0**, while the optimized concentration of glucose, 1 mM, and soluble O_2, being in equilibrium with air, were defined as the logic value **1**. The whole biomolecular system, which accepts four input signals, anti-DNP (**A**), anti-NT (**B**), glucose (**C**), and O_2 (**D**), can be represented by an equivalent logic circuitry composed of three concatenated logic gates, Scheme 2. Immune-selective input signals **A** and **B** applied to the antigen-functionalized surface result in the attachment of the biocatalytic tag (HRP) only if at least one of the primary antibodies is bound to the surface (combinations of the input signals **A** and **B**: **0**,**1**; **1**,**0**; **1**,**1**), while in the absence of the both primary antibodies (input signal combination **0**,**0**), the biocatalytic tag is not bound to the antigen film. Considering the appearance of the biocatalytic HRP tag as the output signal of the gate (consistent

SCHEME 2: Logic Network Composed of Concatenated Gates Activated by Antibodies and Enzyme Substrates Used As Input Signals

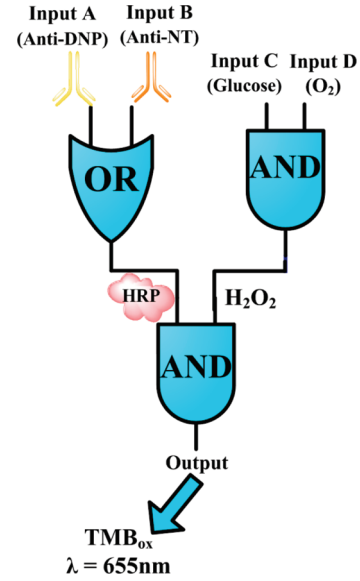

with the AFM measurements described above), the first logic operation made on the system resembles the Boolean **OR** operation. Operating in parallel, GOx produces H_2O_2 as the output signal only in the presence of the both reacting inputs glucose and O_2 (input signal combination **1**,**1**), while in the absence of either of them or both of them (input signal combinations **0**,**1**; **1**,**0**; **0**,**0**), the biocatalytic system stays mute. Thus, the response of the system to the inputs corresponds to the Boolean **AND** logic operation. The next reaction step, when TMB is biocatalytically oxidized to yield the optical output signal (absorbance increase at $\lambda = 655$ nm), Figure 3, proceeds only when the intermediate output signals from the preceding **OR**/**AND** logic gates have a value of **1**,**1** (in other words, in the presence of the HRP biocatalytic tag and H_2O_2), thus resembling the final **AND** logic operation, Scheme 2.

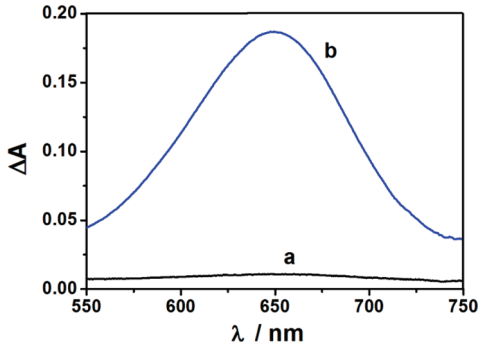

Figure 3. Sample spectra generated by the immune logic system upon the input signal combinations of **0**,**0**,**0**,**0** (a) and **1**,**1**,**1**,**1** (b). The exact composition of the logic gates and the definition of the biochemical signals are given in the Experimental Section.

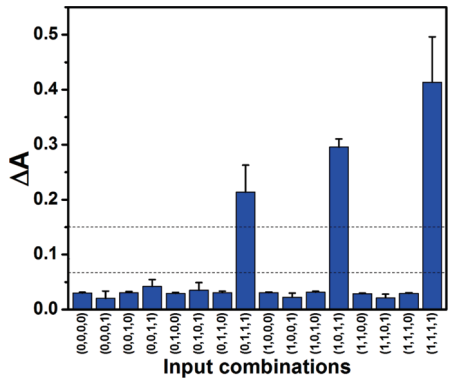

Figure 4. Optical output generated by the immune enzyme logic network as a function of the 16 possible input signal combinations. Dash lines show the thresholds separating the digital **0** and **1** output signals produced by the system. The exact composition of the logic gates and the definition of the biochemical signals are given in the Experimental Section.

The final output signals, recorded optically as the absorbance changes due to the TMB biocatalytic oxidation, were analyzed for all 16 combinations of four input signals (two of them corresponding to the immune interactions and two other corresponding to the biocatalytic reactions). Figure 4 shows the pattern of the generated output signals, where output **1** was observed at the **0**,**1**,**1**,**1**; **1**,**0**,**1**,**1**; and **1**,**1**,**1**,**1** combinations of the inputs, while all other combinations of the inputs yielded the output **0**. The whole set of the output signals originating from the different input combinations is also presented in the truth table (Table 1) corresponding to the experimental data shown in Figure 4. It should be noted that the truth table perfectly correlates with the expected logic performance of the network shown in Scheme 2.

Conclusions and Perspectives

The studied system has demonstrated the possibility to logically process immune-specific interactions, coupled with enzyme-based logic networks activated by biochemical signals. The new approach to multisignal biosensing allows qualitative evaluation of the biochemical information in terms of **YES**−**NO**, providing the background for the logic analysis of complex patterns of biochemical signals. Stable information processing with clearly distinguishable output signals from different combinations of biochemical input signals of various natures was achieved. Application of AFM for the signal transduction in the immune logic systems allows tremendous miniaturization of the signal processing systems, bringing them to a microsize level.

TABLE 1: Truth Table for the Logic Network Based on the Concerted Operation of the Immune-Specific and Biocatalytic System Triggered by Anti-DNP, Anti-NT, Glucose, and Oxygen Producing an Optical Output Signal[a]

input A (anti-DNP)	input B (anti-NT)	input C (glucose)	input D (O_2)	output (ΔA at λ = 655 nm)
0	**0**	**0**	**0**	**0**
0	**0**	**0**	**1**	**0**
0	**0**	**1**	**0**	**0**
0	**0**	**1**	**1**	**0**
0	**1**	**0**	**0**	**0**
0	**1**	**0**	**1**	**0**
0	**1**	**1**	**0**	**0**
0	**1**	**1**	**1**	**1**
1	**0**	**0**	**0**	**0**
1	**0**	**0**	**1**	**0**
1	**0**	**1**	**0**	**0**
1	**0**	**1**	**1**	**1**
1	**1**	**0**	**0**	**0**
1	**1**	**0**	**1**	**0**
1	**1**	**1**	**0**	**0**
1	**1**	**1**	**1**	**1**

[a] The definitions of the digitized input and output signals are given in the text.

Besides fundamental interest in biocomputing logic systems, the present approach will allow logic processing of immune signals in various biomedical applications. The developed approach opens the way to novel fully chemical digital biosensors processing biochemical information and producing an output signal dependent on the whole pattern of various input signals. The output signal might be directed to chemical actuators (e.g., signal responsive membranes or capsules), leading to an on-demand drug release. We anticipate that such biochemical logic gates composed of immune recognition and biocatalytic systems will facilitate decision making in connection to an autonomous feedback loop drug delivery system and will revolutionize the monitoring and treatment of patients with various medical problems.

Additional important steps waiting to be studied are as follows: (i) Further increase of the immune enzyme logic complexity is needed for the future integration of biomedical devices with natural in vivo biochemical environments. (ii) The immune enzyme systems processing biochemical signals should be directly immobilized on the signal-transducing electronic interfaces or stimuli-activated chemical actuators (e.g., switchable membranes). These studies are in progress in our laboratories, including integration of immune logic systems with bioelectronic devices, for example, with biofuel cells.[18]

Acknowledgment. We gratefully acknowledge support of our research programs by the National Science Foundation (Grants CCF-0726698, CBET-0755704, and DMR-0706209), by the Office of Naval Research (Grant N00014-08-1-1202), and by the Semiconductor Research Corporation (Award 2008-RJ-1839G). This research in part was supported by the Nanoengineering and Biotechnology Laboratories Center (NABLAB), Clarkson University. G.S. acknowledges a Wallace H. Coulter Scholarship at Clarkson University.

Supporting Information Available: Preparation of the nitrotyrosine−BSA conjugate and optimization of the logic input values. This material is available free of charge via the Internet at http://pubs.acs.org.

References and Notes

(1) (a) Shao, X. G.; Jiang, H. Y.; Cai, W. S. *Prog. Chem.* **2002**, *14*, 37–46. (b) Saghatelian, A.; Volcker, N. H.; Guckian, K. M.; Lin, V. S. Y.; Ghadiri, M. R. *J. Am. Chem. Soc.* **2003**, *125*, 346–347. (c) Ashkenasy, G.; Ghadiri, M. R. *J. Am. Chem. Soc.* **2004**, *126*, 11140–11141.

(2) (a) De Silva, A. P.; Uchiyama, S. *Nat. Nanotechnol.* **2007**, *2*, 399–410. (b) Credi, A. *Angew. Chem., Int. Ed.* **2007**, *46*, 5472–5475. (c) Pischel, U. *Angew. Chem., Int. Ed.* **2007**, *46*, 4026–4040.

(3) (a) Sivan, S.; Lotan, N. *Biotechnol. Prog.* **1999**, *15*, 964–970. (b) Sivan, S.; Tuchman, S.; Lotan, N. *Biosystems* **2003**, *70*, 21–33. (c) Deonarine, A. S.; Clark, S. M.; Konermann, L. *Future Generation Computer Systems* **2003**, *19*, 87–97. (d) Ashkenazi, G.; Ripoll, D. R.; Lotan, N.; Scheraga, H. A. *Biosens. Bioelectron.* **1997**, *12*, 85–95. (e) Unger, R.; Moult, J. *Proteins* **2006**, *63*, 53–64.

(4) (a) Stojanovic, M. N.; Stefanovic, D.; LaBean, T.; Yan, H. In *Bioelectronics: From Theory to Applications*; Willner, I., Katz, E., Eds.; Wiley-VCH: Weinheim, Germany, 2005; pp 427−455. (b) Saghatelian, A.; Volcker, N. H.; Guckian, K. M.; Lin, V. S. Y.; Ghadiri, M. R. *J. Am. Chem. Soc.* **2003**, *125*, 346–347. (c) Ashkenasy, G.; Ghadiri, M. R. *J. Am. Chem. Soc.* **2004**, *126*, 11140–11141.

(5) Win, M. N.; Smolke, C. D. *Science* **2008**, *322*, 456–460.

(6) Simpson, M. L.; Sayler, G. S.; Fleming, J. T.; Applegate, B. *Trends Biotechnol.* **2001**, *19*, 317–323.

(7) Xu, J.; Tan, G. J. *J. Comput. Theor. Nanosci.* **2007**, *4*, 1219–1230.

(8) (a) Zhou, J.; Tam, T. K.; Pita, M.; Ornatska, M.; Minko, S.; Katz, E. *ACS Appl. Mater. Interfaces* **2009**, *1*, 144–149. (b) Privman, M.; Tam, T. K.; Pita, M.; Katz, E. *J. Am. Chem. Soc.* **2009**, *131*, 1314–1321. (c) Pita, M.; Katz, E. *J. Am. Chem. Soc.* **2008**, *130*, 36–37.

(9) Krämer, M.; Pita, M.; Zhou, J.; Ornatska, M.; Poghossian, A.; Schöning, M. J.; Katz, E. *J. Phys. Chem. B* **2009**, *113*, 2573–2579.

(10) (a) Tam, T. K.; Pita, M.; Ornatska, M.; Katz, E. *Bioelectrochemistry* **2009**, doi: 10.1016/j.bioelechem.2009.03.008. (b) Amir, L.; Tam, T. K.; Pita, M.; Meijler, M. M.; Alfonta, L.; Katz, E. *J. Am. Chem. Soc.* **2009**, *131*, 826–832.

(11) (a) Tokarev, I.; Gopishetty, V.; Zhou, J.; Pita, M.; Motornov, M.; Katz, E.; Minko, S. *ACS Appl. Mater. Interfaces* **2009**, *1*, 532–536. (b) Motornov, M.; Zhou, J.; Pita, M.; Tokarev, I.; Gopishetty, V.; Katz, E.; Minko, S. *Small* **2009**, *5*, 817–820. (c) Pita, M.; Krämer, M.; Zhou, J.; Poghossian, A.; Schöning, M. J.; Fernández, V. M.; Katz, E. *ACS Nano* **2008**, *2*, 2160–2166. (d) Motornov, M.; Zhou, J.; Pita, M.; Gopishetty, V.; Tokarev, I.; Katz, E.; Minko, S. *Nano Lett.* **2008**, *8*, 2993–2997. (e) Pita, M.; Minko, S.; Katz, E. *J. Mater. Sci.: Mater. Med.* **2009**, *20*, 457−462.

(12) (a) Strack, G.; Pita, M.; Ornatska, M.; Katz, E. *ChemBioChem* **2008**, *9*, 1260–1266. (b) Baron, R.; Lioubashevski, O.; Katz, E.; Niazov, T.; Willner, I. *Org. Biomol. Chem.* **2006**, *4*, 989–991. (c) Baron, R.; Lioubashevski, O.; Katz, E.; Niazov, T.; Willner, I. *J. Phys. Chem. A* **2006**, *110*, 8548–8553. (d) Baron, R.; Lioubashevski, O.; Katz, E.; Niazov, T.; Willner, I. *Angew. Chem., Int. Ed.* **2006**, *45*, 1572–1576.

(13) (a) Strack, G.; Ornatska, M.; Pita, M.; Katz, E. *J. Am. Chem. Soc.* **2008**, *130*, 4234–4235. (b) Niazov, T.; Baron, R.; Katz, E.; Lioubashevski, O.; Willner, I. *Proc. Natl. Acad. Sci. U.S.A.* **2006**, *103*, 17160–17163.

(14) (a) Privman, V.; Strack, G.; Solenov, D.; Pita, M.; Katz, E. *J. Phys. Chem. B* **2008**, *112*, 11777–11784. (b) Privman, V.; Arugula, M. A.; Halámek, J.; Pita, M.; Katz, E. *J. Phys. Chem. B* **2009**, *113*, 5301–5310.

(15) (a) Crowther, J. R. *ELISA: Theory and Practice*; Humana Press: Totowa, NJ, 1995. (b) Crowther J. R. *The ELISA Guidebook*; Humana Press: Totowa, NJ, 2000.

(16) Pita, M.; Cui, L.; Gaikwad, R. M.; Katz, E.; Sokolov, I. *Nanotechnology* **2008**, *19*, 375502.

(17) (a) Sokolov, I. In *Cancer Nanotechnology—Nanomaterials for Cancer Diagnosis and Therapy*; Nalwa, H. S., Thomas Webster, T., Ed.; American Scientific Publishers: Los Angeles, CA, 2007: pp 43−59. (b) Iyer, S.; Gaikwad, R. M.; Subba-Rao, V.; Woodworth, C. D.; Sokolov, I. *Nat. Nanotechnol.* **2009**, *4*, 389–393. (c) Sokolov, I. *Appl. Surf. Sci.* **2003**, *210*, 37–42. (d) Sokolov, I.; Iyer, S.; Subba-Rao, V.; Gaikwad, R. M.; Woodworth, C. D. *Appl. Phys. Lett.* **2007**, *91*, 023902.

(18) Tam, T. K.; Strack, G.; Pita, M.; Katz, E. *J. Am. Chem. Soc.* **2009**, *131*, in press (DOI: 10.1021/ja9048459).

JP905620C